Limnol. Oceanogr., 58(3), 2013, 921–931

doi:10.4319/lo.2013.58.3.0921

Physical responses of small temperate lakes to variation in dissolved organic carbon concentrations

Jordan S. Read,[a,1,*] and Kevin C. Rose[b]

[a] University of Wisconsin–Madison, Department of Civil and Environmental Engineering, Madison, Wisconsin
[b] Smithsonian Environmental Research Center, Edgewater, Maryland

Abstract

We used a mechanistic physical model to examine the effect of variability in dissolved organic carbon (DOC) concentrations on the physical properties of small temperate lakes. The model was validated on eight small (6×10^{-4} to 3.8×10^{-2} km^2) lakes in Wisconsin and Michigan, with a standard error $< 1°C$ for seven of eight lakes. Attenuation of photosynthetically active radiation (400–700 nm) in these lakes was regulated by DOC concentrations and was important in the vertical structuring of water temperatures. Heat exchange below the surface mixed layer was near the molecular rate, increasing the importance of water clarity as a control on the heat content of deeper waters. To understand the thermal effects of changing DOC concentrations, we applied scenarios of a 50% increase and 50% decrease in DOC concentrations for one lake (Trout Bog) and found water temperatures to vary in response, with the seasonally averaged temperatures in the increased DOC scenario being $> 2°C$ colder than the reduced scenario. We found a nonlinear relationship between DOC and temperature, with clearer (lower DOC) simulations being more sensitive to climate variability, suggesting that DOC may act as a buffer against a warming climate. Our model showed that DOC also influenced epilimnetic depths, as nocturnal mixing (related to the vertical partitioning of heat) was more important than wind-driven mixing. Small lakes are globally important regulators of biogeochemical cycles and are structurally different from larger lakes. Important feedbacks to physical processes must be accounted for when understanding the effects of changing DOC and climate on small lakes.

Small lakes (< 0.1 km^2) are globally numerically dominant, especially in temperate latitudes (Downing et al. 2006). These lakes often possess physical and biogeochemical characteristics that differ from larger, more well studied lakes (Downing 2010; Read et al. 2012). Small lakes have large perimeters (relative to their volumetric processing capacity) and consequently are often more heavily subsidized with allochthonous inputs (Cole et al. 2011). Although these lakes make up a small fraction of surface waters (both in area and volume), they are hot spots for biogeochemical cycling (Cole et al. 2007; Downing 2010) and likely play a disproportionately large role in the global carbon cycle.

Physical and biogeochemical characteristics of lakes are changing in response to shifts in regional air temperatures, hydrologic fluxes, and anthropomorphically induced change at the watershed scale (Destasio et al. 1996; Schindler et al. 1996). Lakes can respond to these multiple forcings in complex ways. Lake size can influence physical responses to various drivers; for example, changes in air temperatures and wind speeds may be important for larger lakes, while small lakes might be more responsive to variations in the hydrologic cycle (due to a smaller volumetric buffering capacity). Water transparency may regulate the response of lakes to changes in these drivers, as lakes darkened by high dissolved organic carbon (DOC) concentrations appear to be less sensitive to variations in climate when observed alongside clear water lakes (Snucins and Gunn 2000).

DOC concentration is a primary regulator of many physical, chemical, and biological characteristics of lakes (Kirk 1994; Morris et al. 1995; Fee et al. 1996). High DOC concentrations reduce transparency, which can alter the vertical structure of water temperature and lead to shallower surface mixed layers (Kling 1988; Fee et al. 1996; Persson and Jones 2008). In turn, water temperature and the depth of the mixed layer can significantly influence ecosystem-scale characteristics, such as the processing rates of carbon (Hanson et al. 2011). Many investigators have highlighted long-term changes in lacustrine DOC loading and catchment export (Schindler et al. 1996; Striegl et al. 2005; Zhang et al. 2010). Widespread increases in DOC have been attributed primarily to recovery from acidification (Monteith et al. 2007). Increased precipitation may also increase terrestrial DOC loading to lakes, and anthropogenically induced changes in the volume, timing, and magnitude of extreme precipitation events may also drive regional changes in DOC (Jennings et al. 2010).

Despite a wealth of studies that highlight the relationship between water transparency and the physical properties of lakes (such as epilimnetic depth and water temperature), a large majority of these studies are based solely on empirical observations, and few mechanistic studies have been performed (Persson and Jones 2008). Understanding the mechanisms behind physical change is critical to assessing and quantifying the effects of climate feedbacks and effects on lake ecosystems. With both increasing (Monteith et al. 2007) and decreasing (Striegl et al. 2005) DOC concentrations observed in regions around the world, it is important

* Corresponding author: jread@usgs.gov

[1] Present address: U.S. Geological Survey Center for Integrated Data Analytics, Middleton, Wisconsin

Table 1. Lake properties for the eight lakes used in this analysis.

Lake name	Latitude	Longitude	Surface area ($\times 10^{-2}$ km^2)	Max depth (m)	Buoy type	DOY range	Year
Crystal Bog	46.0076	−89.606	0.55	2.5	1	133–201	2009
Jekl Bog	45.9946	−89.678	0.25	3.1	1	132–173	2011
Mouser Bog	45.9977	−89.722	3.78	4	2	138–195	2011
North Sparkling Bog	46.0048	−89.705	0.46	4.3	1	107–338	2009
Peter	46.2529	−89.504	2.68	18	1	132–246	2011
Timber Bog	46.0034	−89.431	0.06	2	1	132–177	2011
Trout Bog	46.0411	−89.686	1.05	7.9	1	125–321	2009
Ward	46.2548	−89.517	2.01	8.3	2	142–264	2011

DOY, day of year.

to determine the magnitude and direction of physical responses to changes in water transparency and the modulation of these responses due to climate variability.

We focus here on modeling several physical responses of small temperate lakes to changing DOC concentrations because these lakes are numerically dominant and globally important (Downing et al. 2006; Downing 2010). Small lakes play a disproportionately large role in the global carbon budget (Cole et al. 2007; Tranvik et al. 2009), and physical processes are often not well represented when knowledge from larger lakes is scaled down (Read et al. 2012). We mechanistically model the processes that regulate the vertical structure of water temperatures and identify controls on epilimnetic depth and the interannual variability of water temperatures in small lakes. We hypothesize that because small lakes are often convectively dominated (Read et al. 2012), mixed-layer deepening is driven by heat loss, and the vertical structure of water temperature is a function primarily of molecular diffusion of heat and the attenuation of light. Using a one-dimensional hydrodynamic model, we examine the influence of DOC on the physical properties of small temperate lakes, simulate two DOC concentration scenarios in the context of broadly observed long-term changes in DOC, and test the hypothesis that darker lakes will be less sensitive to variation in climate.

Methods

Site description—We included eight instrumented humic lakes in this analysis that were located in northern Wisconsin or in the Upper Peninsula of Michigan in the United States. Lakes ranged in size from 6×10^{-4} to 3.8×10^{-2} km^2, with maximum depths varying from 2 to 18 m (Table 1). These lakes were surrounded with a mixture of low-lying forest cover and catchments with minimal relief. All lakes had low wind speeds, with the highest median wind speed for any of the lakes < 1.3 m s^{-1} (Mouser Bog). While detailed hydrologic measurements exist only for a few lakes in this analysis, none of the lakes have measureable surface inflows or outflows. The hydrologic budgets for these lakes are dominated by precipitation, evaporation, and net groundwater losses. Crystal Bog and Trout Bog are long-term study lakes under the North Temperate Lakes Long-Term Ecological Research Program (http://lter.limnology.wisc.edu), Peter Lake and Ward Lake have been extensively studied and are part of the University of Notre Dame Environmental Research Center, and North Sparkling Bog has been monitored since 2003 as part of the University of Wisconsin–Madison Microbial Observatory. This effort, to the best of our knowledge, is the first detailed study of Jekl, Timber, and Mouser Bogs.

Physical measurements—Lakes were fitted with instrumented buoys for parts of multiple open-water seasons, but we focused on ice-free periods in 2009 and 2011 because these years had supporting optical and chemical surveys. Buoys were of two types. Type 1 buoys had meteorological sensors for measuring wind speed, relative humidity, and air temperature as well as thermistor strings in the water column; type 2 buoys had observations of only wind speed and water temperatures. Type 2 sites assumed that air temperature and relative humidity were equal to measurements made on nearby lakes of similar type (e.g., Peter Lake data were used on Ward Lake, which is approximately 1 km west of Peter). We used a single station (the Noble F. Lee Airport, 45.93°N, −89.73°W) for measurements of incoming solar and terrestrial radiation (Eppley PSP pyranometer and Eppley PIR radiometer, respectively). Estimates of the diffuse attenuation coefficient (K_d) of photosynthetically active radiation (PAR; 400–700 nm) were made with observations of the depth-decay of PAR using a profiling radiometer (Biospherical Instruments Inc. These measurements were taken near the start of each observation period and averaged with periodic profiles from the following months to create a seasonal average (with the exception of Ward and Peter Lakes, which were measured only once). K_d was estimated according to the relationship

$$E_z - E_0 \exp(-K_d \times z) \quad (1)$$

where E_z is PAR irradiance at a given depth (z) and E_0 is PAR irradiance at the surface. Diffuse attenuation coefficient estimates were made using PAR measurements taken between depths of 50–1% of E_0, or the depth of 50% of E_0 to the maximum measurement depth (in cases where the depth of 1% E_0 was greater than the depth of the lake). Occasionally, this depth range incorporated non–log linearity in attenuation (likely due to photobleaching of DOC in the surface mixed layer), which increased uncertainty in these estimates. Integrating over this depth range provided a more representative average whole water column K_d as opposed to augmenting our fitting range to include only the log-linear portion of measurements.

During the summer of 2010, a self-contained automated microstructure profiler (SCAMP; Precision Measurement Engineering) was used to measure the fine-scale distribution of water temperatures in Trout Bog. We used the SCAMP in upward profiling mode. The SCAMP sampled at 100 Hz and ascended at 10 cm s^{-1}, yielding approximately a 1 mm vertical resolution for temperature measurements.

Lab methods—Samples for DOC concentration and chlorophyll *a* (Chl *a*) were collected from eight lakes (including three of the instrumented lakes) in northern Wisconsin in October 2009 to understand what regulated variability in PAR K_d among lakes in this region and to characterize the DOC : K_d ratio of small temperate bog lakes. These samples were taken near the same time as supporting light profiles. DOC was measured with three replicate samples collected from within the surface mixed layer (1–3 m). We report the mean of the three replicates. Samples were collected, immediately filtered through 0.7 μm Whatman GF/F filters, and stored in the cold and dark until analysis. DOC concentration was measured using a Shimadzu total organic carbon analyzer (model Vcph). DOC was measured in standard sensitivity mode, and we subtracted Milli-Q deionized water blanks (~ 0.2 mg C L^{-1}) from standards and samples and calibrated to dilutions of a certified DOC standard (Aqua Solutions; 50 mg L^{-1} potassium biphthalate).

Chl *a* concentrations were collected with two replicate samples from within the surface mixed layer (1–3 m). Water was filtered through preashed 0.7 μm Whatman GF/F filters, and filters were folded, wrapped in foil, and frozen until analysis immediately on returning from the field. Chlorophyll was extracted using an acetone–methanol mixture, and the extract was clarified by centrifugation following the methods of Pechar (1987). Chl *a* concentrations were determined fluorometrically after correcting for the presence of phaeopigments.

Measurements of DOC from the North Temperate Lakes Long-Term Ecological Research (NTL-LTER) program were pooled over the depth range of 0–3 m measured during the ice-free period of Trout Bog for each year from 1989 to 2010. This depth range bounded the range used to estimate PAR K_ds in optical measurements in Trout Bog. Measurements of DOC were typically made monthly during the ice-free period, with varying depths and numbers of replicates for each depth. We used the total measurements for each ice-free season (that were in the specified depth range) to calculate the median annual DOC concentration.

We modeled the physical response of lakes to several DOC scenarios, including baseline (the measured DOC concentration) and a 50% increase and a 50% decrease in DOC concentration in Trout Bog. We assumed that these changes in DOC altered water column transparency relative to our derived DOC specific attenuation coefficients.

Water temperature model—We used a one-dimensional physical water temperature model to simulate water temperatures and mixing dynamics in small sheltered lakes, where convective mixing is typically greater in magnitude than wind-driven mixing (Read et al. 2012). The model, referred to as the convective lake model (CLM), uses a vertical distribution of mixed layers and iteratively calculates the changes in energy (and corresponding changes in temperature) of the layers for each time step. Surface energy fluxes, the attenuation of shortwave energy in the water column, as well as surface mixing dynamics, such as wind shear and convection, are included in the model, but surface-water flows, groundwater fluxes, and changes in lake levels are not. An earlier version of the model is described elsewhere (Read et al. 2011) and differs from many common water temperature models (Imberger and Patterson 1981) in that CLM was designed and calibrated for small temperate lakes. In brief, the model calculates the net surface energy flux (Q_0) as

$$Q_0 = R_{\mathrm{net}} - E - H \tag{2}$$

where R_{net} is the sum of surface radiation, E is the latent heat flux, and H is the sensible heat flux. R_{net} includes the net of incoming long-wave radiation, outgoing long-wave radiation (parameterized according to the Stefan–Boltzman relationship for the water surface temperature radiating at 97.2% emissivity), and the portion of shortwave radiation that is directly absorbed in the near-surface layer (assumed to be 55% of nonreflected radiation, where the remaining energy fraction of the shortwave spectrum penetrates into the water column and is attenuated below the near-surface layer). For long-wave and shortwave radiation, we assumed albedos of 3% and 7%, respectively. E and H were calculated according to the additive air-side renewal processes of both buoyancy flux and wind (Rasmussen et al. 1995). We used the Rasmussen et al. (1995) model because these small lakes lack developed atmospheric boundary layers, violating the assumptions required to parameterize E and H based on common bulk aerodynamic transfer coefficients.

These surface energy fluxes are then summed and applied to the temperature of the near-surface layer. The remaining radiation is attenuated according to the simulation value of K_d, where the depth loss of radiation in Eq. 1 (applying incremental steps to z for each vertical layer of the model) is converted to thermal energy (i.e., a temperature increase) for each vertical layer. We parameterized K_d with a single bulk coefficient, approximated by PAR K_d, because previous studies have shown that the wavelengths shorter than PAR (400–700 nm) contribute only a few percent to the thermal energy gain below the near-surface layer (Kirk 1994), and our radiometer measurements showed that in all modeled lakes, over 99% of ultraviolet radiation was attenuated within the upper 80 cm (data not shown). Water molecules strongly absorb wavelengths longer than 700 nm, rapidly attenuating these wavelengths in the near-surface layer (Kirk 1994). Next, the surface mixed layer (z_{mix}) is propagated downward relative to the strength of wind shear and convective heat loss vs. the ambient stratification (Imberger 1985). This process mixes the available thermal energy between all layers above z_{mix}. Next, the model applies an eddy diffusion flux (K_z) of thermal energy at the division between all layers, incrementing or decrementing layer temperatures relative to the thermal gradient between neighbors. These processes are applied iteratively at each time step (in this order) for the duration of each simulation.

We used CLM to examine the roles of both K_z and K_d in the vertical structuring of water temperatures in the study lakes using two methods. First, we used two SCAMP temperature profiles from Trout Bog that were separated by 40 d in the summer of 2010 to partition heat gains (or losses) attributed to K_z compared to the temperature increases from the vertical attenuation of penetrating radiation (the role of K_d). We used an hourly time step of CLM and iterated through values for K_z and K_d to minimize the sum of squared errors between modeled and observed heat gains in 10 cm intervals. Only measurements below the maximum nocturnal mixed-layer depth were used for this optimization (a maximum of 1.6 m during the 40 d). Second, we used the entire buoy observation period for each of the eight lakes and iterated through realistic potential ranges of K_z and K_d to minimize the sum of squared errors between thermistor measurements and CLM hourly modeled temperatures at the same depths (excluding surface thermistors). For both of these methods, the CLM starting water temperatures were initialized with the first observed water column profile (SCAMP or buoy thermistor string), and linear interpolation was used when necessary for the initialization (when temperature observations were coarser than model layers).

Modeling scenarios—Trout Bog has a long-term record of physical, chemical, and biological observations that began in 1981. Meteorological measurements at the Noble F. Lee Airport were added to the NTL-LTER program in 1989, providing a period of more than 20 yr where routine measurements can be coupled with a physical model of Trout Bog. For all years from 1989 to 2010, we used NTL-LTER observations ice-on and ice-off dates, DOC concentrations, and meteorological driver data to simulate open-water temperatures for Trout Bog. After simulating and adjusting the model for size-specific parameters, such as the wind sheltering coefficient (Markfort et al. 2010), we randomized yearly DOC concentrations (holding the derived relationship between DOC and K_d constant), and randomly iterated through simulation years. This process was repeated for 1000 simulations, and we calculated the volumetric average water temperature for each simulation. We also used two DOC change scenarios: a 50% increase and a 50% decrease in yearly DOC concentrations. These scenarios were applied to the randomized DOC choice of the "baseline" case, resulting in 3000 total simulations and corresponding estimates of average water temperatures.

To test the hypothesis that clearer lakes are more sensitive to climate variability, we modeled water temperatures for 15 hypothetical lakes that varied in DOC concentrations (from 2 to 30 mg L^{-1}) but were otherwise identical to Trout Bog. Using the climate driver data and modeling effort described above, we modeled water temperatures for each open-water period, calculating the volumetrically averaged temperature for all 22 seasons and 15 model lakes. Using the resulting water temperatures, we calculated the temperature range for each model lake as the difference between the warmest and coldest temperatures. This temperature range provided a metric for comparing the physical variability in each model lake that would result from the inherent climate variations of the 22 unique simulation years.

Statistical methods—K_d was estimated by fitting depth-dependent measurements of PAR to an exponential decay curve (*see* Eq. 1). We used raw data for K_d fitting (instead of log-transforming irradiance observations and using a linear regression) because we wanted an accurate representation of uncertainty in K_d. For these exponential fits, we applied an algorithm that minimized nonlinear least squares for irradiance and depth data (MATLAB's fit.m function, http://mathworks.com). Both K_d and E_0 were treated as unknowns for this optimization routine. We also calculated 95% confidence intervals for the fit of K_d.

A stepwise multiple linear regression analysis was used to test if DOC concentration and Chl *a* concentration were significant predictors of PAR K_d in the eight lakes where these measurements were made. Based on the results from this analysis, we estimated DOC-specific PAR attenuation coefficients by dividing PAR K_ds by DOC concentrations in the three bog lakes (Trout Bog, Crystal Bog, and North Sparkling Bog). DOC-specific PAR attenuation coefficients assume that DOC is the only significant regulator of PAR K_d in these systems. This assumption allowed us to estimate the total PAR attenuation contribution of DOC independent of wavelength-specific absorption coefficients or other potential attenuating substances.

Estimates for modeled K_z and K_d for each of the simulated lakes were obtained using a minimization routine to determine the "best fit" between simulations and observations. For simulations, CLM was initialized using the first observation of water temperatures, and simulations included the total duration between the first and last thermistor measurements for the calendar year. For some lakes, intermittent instrument errors caused a short-term loss of observations. To avoid artificially changing the error structure, we did not interpolate these missing periods. Instead, we compared actual buoy observations to our model output only when both existed. CLM simulated water temperatures at a finer resolution than thermistors, so we extracted the model depths that matched the depths of in situ observations and calculated the total sum of squared errors for all matched depths (except the near-surface thermistor). Our minimization routine minimized this total error quantity across values for K_z and K_d. We calculated standard errors for each of these simulations following the same procedures as Rasmussen et al. (1995).

Results

Across the eight lakes sampled, variation in PAR K_d was a first-order function of variation of DOC concentrations

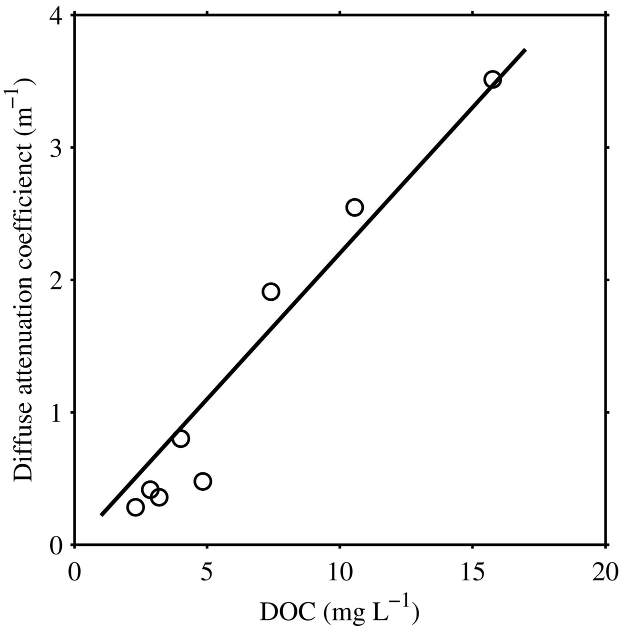

Fig. 1. Relationship between the diffuse attenuation coefficient (K_d) and DOC for seven NTL-LTER lakes and North Sparkling Bog from a 2009 survey. Solid line represents the linear function with slope = 0.22.

(Fig. 1; $p < 0.01$, $R^2 = 0.95$). Holding the y-intercept at zero, the slope of the linear model predicting PAR K_d from DOC concentrations was 0.217 ($\pm$ 0.04). Adding variation in Chl *a* concentration to this model did not significantly improve model fit. Among the three bog lakes that were sampled, the average DOC-specific PAR K_d was 0.232 m^{-1} mg^{-1} L ($\pm$ 0.04). We used the relationship between attenuation and DOC concentration proposed by Morris et al. (1995) (0.22 m^{-1} mg^{-1} L, which is also the approximate mean of these two estimates) to estimate K_d per unit (mg L^{-1}) of DOC for scenario (+50% and −50%) and baseline concentrations of DOC.

We found heat transfer below the mixed layer to occur at a molecular or near-molecular rate (Fig. 2). Changes in hypolimnetic temperatures during the 40 day period between profiles on Trout Bog were explained by summing the effects of vertical diffusion of heat (best fit for K_z was 1.5×10^{-7} m^2 s^{-1}) and the attenuation of penetrating radiation (best fit for K_d was 2.2 m^{-1}). CLM was fit to the buoy-based observation data by simulating water temperatures across a range of K_d and K_z values, and the best model performance for all eight lakes was achieved by limiting K_z to the molecular level of 1.4×10^{-7} m^2 s^{-1} (Fig. 2; Table 2). Minimizing the difference between modeled and observed data resulted in best-fit estimates of K_d that were within 10% of field estimates for five of the eight lakes (Table 2). Two notable exceptions were Crystal Bog and Ward Lake, where differences between modeled and observed K_d were approximately 50%. The other exception was North Sparkling Bog. Excluding Crystal Bog and Ward Lake, all modeled estimates of K_d were slight underestimates of field K_d.

CLM performed well in the simulations of water temperature for the eight lakes. Seven of the eight lakes had a standard error (SE) between simulations and observations of less than 1°C, and the worst fit was obtained on the largest, windiest lake (SE: 1.28°C; Mouser Bog). Trout Bog had the lowest model error (0.37°C) and the best agreement between field and model estimates of K_d (Fig. 3; Table 2).

Because attenuation was strongly regulated by DOC in these systems (Fig. 1), modeled increases and decreases in

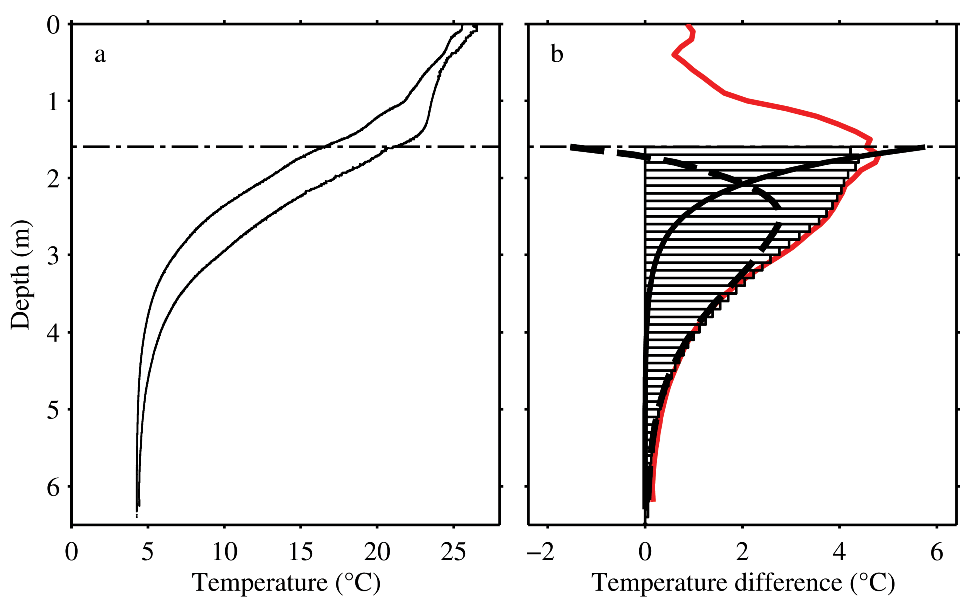

Fig. 2. (a) Temperature profiles on Trout Bog separated by 40 d. (b) Temperature gains are shown as averages for 10 cm intervals (red line). Modeled temperature gains for depths below the remnant mixed-layer depth are shown as 10 cm bins, which combine the additive effects of temperature gains and losses from the vertical diffusion of heat (dashed black line) and the attenuation of penetrating radiation (thick black line).

Table 2. Simulation results for eight sheltered lakes. Model K_d is the best fit to the observed data if K_d is treated as an unknown, observed K_d is a single-point estimate of PAR K_d taken during the observation year, 95% confidence intervals (CIs) are from nonlinear least-squares fits to the exponential decay of light, and SE is the standard error between all observed and modeled water temperatures with the exception of surface thermistors.

Lake name	Model K_d (m^{-1})	Observed K_d (m^{-1})	K_d 95% CI (m^{-1})	SE (°C)
Crystal Bog	3.62	2.55	2.51–2.58	0.73
Jekl Bog	1.85	1.93	1.91–1.94	0.75
Mouser Bog	2.46	2.54	2.48–2.60	1.28
North Sparkling Bog	1.6	1.91	1.88–1.94	0.84
Peter	0.84	0.93	0.89–0.97	0.70
Timber Bog	1.72	1.83	1.8–1.86	0.96
Trout Bog	3.5	3.51	3.41–3.62	0.37
Ward	2.58	1.66	1.59–1.75	0.66

DOC concentrations had a substantial effect on the vertical distribution of water temperatures. Increased transparency (decrease in K_d) occurred in our scenario where DOC concentrations were reduced (as we assumed K_d to be a function of DOC), which resulted in a warmer hypolimnion compared to baseline and DOC increase scenarios. Volume-weighted seasonally averaged water temperatures for lower DOC scenarios were in excess of 2°C warmer compared to the increased DOC scenarios (Fig. 4), although near-surface temperatures generally increased with higher DOC concentrations for much of the season (data not shown).

We used CLM to compare the effects of transparency as a control on the interseasonal variability in water temperatures. The range between the warmest and the coldest temperatures resulting from 22 unique simulation years was greater in lakes with lower DOC concentrations (Fig. 5a). Clearer simulations (i.e., 2 mg L^{-1}) had nearly a 3°C temperature range between the warmest and coldest simulation years. For greater concentrations of DOC, this temperature range was reduced by almost 50%. Thus, CLM provides model support to our hypothesis that darker lakes are less sensitive to climate variability. To provide a reference to these changes, we compared the thermal effects of climate variability to variations in yearly DOC concentrations in Trout Bog. Again, we found that high DOC led to less thermal variability, where higher DOC (i.e., the 15–25 mg L^{-1} range, which would characterize Trout Bog) simulations during 1989–2010 led to similar variability in temperatures when compared to the range of DOC concentrations observed during the same time period (Fig. 5b). For example, fixing the DOC concentration at 20 mg L^{-1} and calculating the average temperatures for the 22 simulation seasons resulted in a range of 1.57°C. By holding the simulation year constant and varying DOC

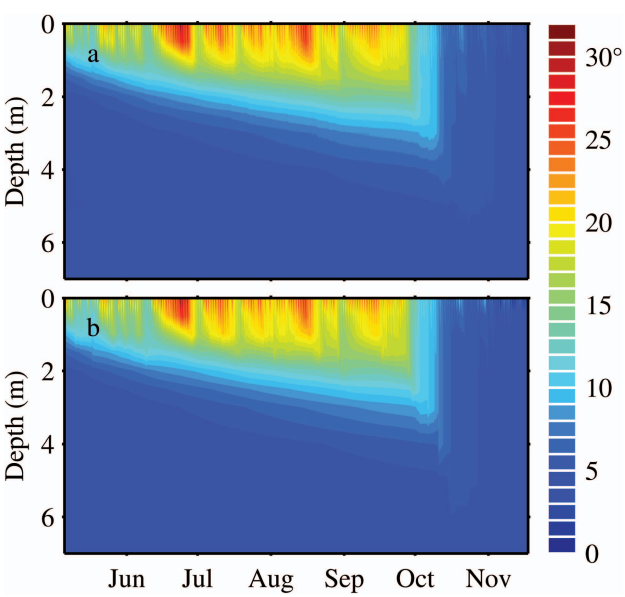

Fig. 3. (a) Observed and (b) modeled temperatures for Trout Bog during 2009. Contour intervals represent 1°C.

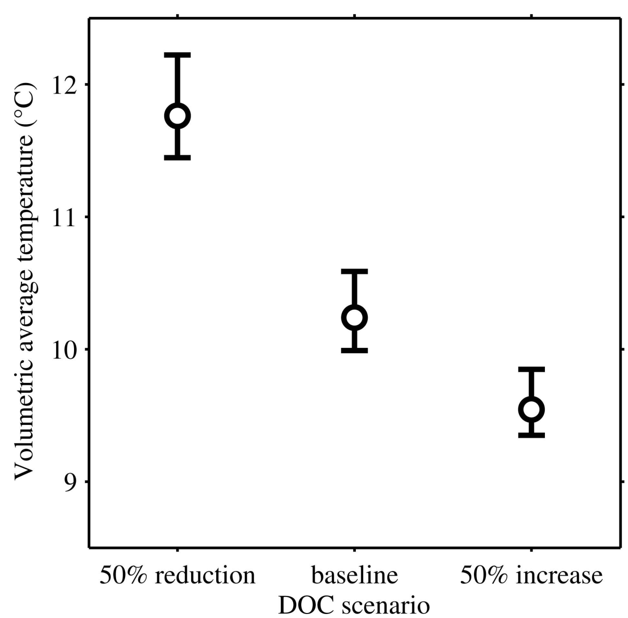

Fig. 4. Volumetric average water temperatures for 22 simulation years and three DOC scenarios for Trout Bog. 1000 iterations were used where DOC concentrations were randomly chosen (with replacement) from the 22 yr on record, and the simulation years were also chosen the same manner (*see* Table 3). Medians are represented by open circles, and error bars represent the interquartile range for all iterations.

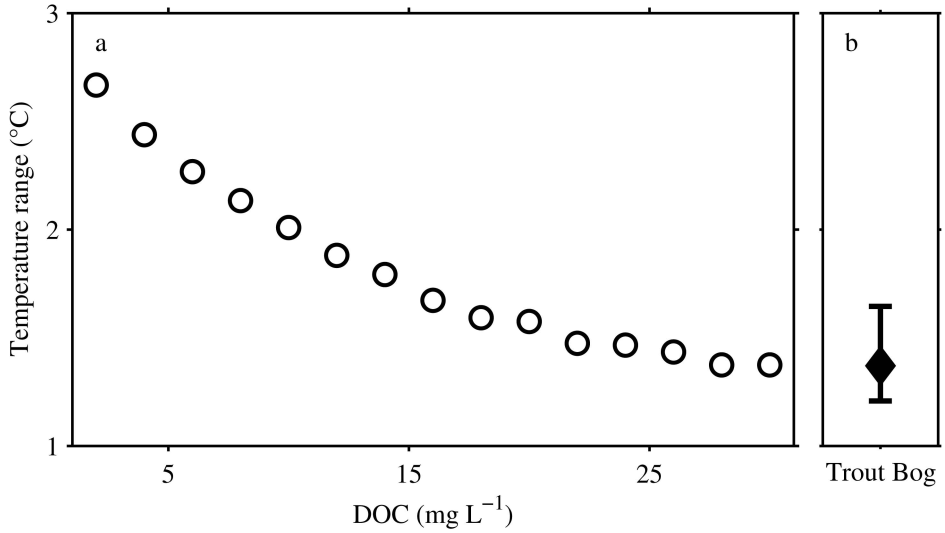

Fig. 5. (a) A model lake with the morphometry of Trout Bog was simulated for a range of DOC concentrations (2–30 mg L^{-1}) to assess the sensitivity of water temperature to natural climate variability (1989–2010). Temperature range was calculated as the difference between maximum and maximum volumetric average temperatures for all 22 seasons (open circles). (b) We calculated the DOC-induced temperature variability for Trout Bog, where we simulated water temperatures for a given year over the full range of DOC 1989–2010 concentrations measured in Trout Bog (Table 3). Each of 22 simulation years had a range between the maximum and minimum average temperatures; the median of this range is plotted as a black diamond, and error bars represent the minimum and maximum range of all years (which were 2009 and 2003, respectively).

based on observations (Table 3), we calculated temperature ranges for each season based solely on the range of DOC concentrations. The median of these ranges was 1.37°C, with a maximum and minimum of 1.65 and 1.21, respectively (simulation years 2003 and 2009).

Discussion

We found that the vertical exchange of heat below the mixed layer occurred at (or near) the rate of molecular diffusion in these lakes (Fig. 1; Table 2) and that DOC concentrations (as the primary driver of K_d) strongly influenced water temperatures, outward heat fluxes, and mixed-layer depths. Because diffusive heat transfer at the molecular rate is slow, water temperatures were highly sensitive to variability in attenuation. Many authors have found relationships between water color and the physical properties in lakes (such as stratification and thermocline depth) that weakened with increasing lake size (Mazumder and Taylor 1994; Fee et al. 1996). We hypothesize that this finding is due to increased K_z on larger lakes, which could effectively mute the influence of variations in K_d. In contrast with large lakes, vertical water temperature profiles in the small lakes studied here resembled the exponential curves of decaying light (Fig. 1), a pattern that was also observed by Fee et al. (1996) in many small Canadian Shield lakes. This finding highlights the importance of color in driving the thermal structure of small, sheltered lakes and suggests that the shape of the temperature–depth relationship characterizes the relative importance of K_d vs. K_z as regulators of thermal structure.

Actual and modeled K_d differed by less than 10% in most lakes, which highlights the success of this relatively simple hydrodynamic model. Variation between modeled K_d and actual K_d was expected because our mechanistic model did not include all components that have influence on the thermal structure of lakes (e.g., groundwater fluxes). Modeled K_ds in Crystal Bog were greater than expected, perhaps because heat flux from the shallow water column into sediments (a minor heat loss term that can be important for shallow lakes but was not considered in this model) required an artificial amplification of K_d to improve the fit between modeled temperature and observations. This was not an issue in the other shallow bog (Timber Bog), likely due to a shorter simulation period that was biased toward the beginning of the season, when water and sediment temperatures would be similar (Table 1). The large difference between modeled and measured K_d in Ward Lake may be due to large seasonality in K_d that was not measured in situ. Ward Lake increased in DOC from 7 to 15 mg L^{-1} in 2010 during a period similar to the length of our deployment (R. Batt pers. comm.), and our only in situ measurement of K_d was taken several days before the buoy was deployed. Performing simulations on shorter periods for Ward Lake supported this hypothesis, as the modeled K_d for only the first 30 d of the observation was much closer to our measurement (1.82 and 1.66, respectively) than the K_d estimated with the entire record (Table 2). This subsampling effort highlighted a trend of increasing K_d over time in Ward Lake (data not shown).

We modeled K_d purely as a function of DOC and used a DOC-specific K_d of 0.22 m^{-1}. The colored, or

Table 3. DOC measurements and modeling details for 1989–2010. Ice-on and ice-off values are the day of year for the first and last observed open water on Trout Bog for the observation year. DOC (mg L^{-1}) values are the median of all measurements made between and including 0 and 3 m, and K_d (m^{-1}) was estimated from DOC measurements using the DOC-specific attenuation coefficient.

	1989	1990	1991	1992	1993	1994	1995	1996	1997	1998	1999	2000	2001	2002	2003	2004	2005	2006	2007	2008	2009	2010
Ice-off	116	113	109	120	118	110	117	130	119	101	105	95	113	114	113	112	105	103	108	121	112	90
Ice-on	317	327	305	316	309	327	311	314	316	341	328	322	340	317	311	328	325	333	319	322	334	327
DOC	13.5	14.8	20.2	20.5	19	18.7	21.2	21.3	20.9	21.8	21	22.6	23.3	23.9	27.5	23.5	24.8	21.8	19.6	18.7	17.4	16
K_d	2.97	3.25	4.45	4.5	4.18	4.12	4.67	4.69	4.59	4.8	4.62	4.98	5.13	5.25	6.04	5.16	5.45	4.8	4.3	4.11	3.82	3.53

chromophoric, portion of DOC is responsible for regulating attenuation in most systems (Morris et al. 1995; Rose et al. 2009*b*). Our use of 0.22 m^{-1} to characterize the unit-specific DOC contribution to attenuation is similar to other estimates, but DOC-specific attenuation may be region specific (Williamson et al. 1996). For example, Morris et al. (1995) identified a DOC-specific contribution to PAR K_d of 0.22 m^{-1}, while other investigators used a coefficient of 0.24 m^{-1} (Perez-Fuentetaja et al. 1999). In the systems we studied here, we assumed that chlorophyll did not contribute to attenuation because our stepwise regression analysis showed that chlorophyll was not a significant predictor of PAR K_d. However, researchers have found that chlorophyll has an influence on PAR attenuation, and Morris et al. (1995) found a Chl *a*–specific contribution of 0.07 m^{-1}. Reductions in DOC may stimulate greater primary production and chlorophyll, while increasing DOC may reduce chlorophyll through shading (Carpenter et al. 1998). If we had included a contribution from Chl *a* for PAR K_d, our modeled changes in DOC would contribute slightly less to changes in K_d.

Darker lakes were generally colder (when compared to the clearer simulations) even though the simulations were driven by the same meteorological observations. Volumetrically colder lakes have less internal energy storage compared to a morphometrically equal warmer lake (thermal energy is proportional to temperature). We used identical incoming radiative inputs for both increased and decreased DOC scenarios. As a result, the colder (darker) simulations had larger outward fluxes of energy in order to satisfy the conservation of energy between scenarios. Our simulations revealed that the largest energy flux variant across the range of DOC concentrations was the outward flux of radiation from the water surface (data not shown). Colder, darker simulations, in general, had warmer surface temperatures compared to more transparent simulations. This higher surface temperature in high-DOC scenarios increased the rate of outward radiation from the water surface, and these fluxes were more important to balancing the previously mentioned water temperature energy deficit than variations in the sum of sensible and latent heat fluxes (data not shown).

It has been hypothesized that transparent lakes (e.g., alpine lakes) may be more sensitive indicators of climate than stained lakes because even small changes in energy, water chemistry, or precipitation may result in large changes in transparency, physical structure, and ecosystem linkages (Snucins and Gunn 2000; Rose et al. 2009*a*). We mechanistically tested this hypothesis by comparing the temperature variability of 22 open-water seasons for model lakes that were morphometrically identical to Trout Bog. Our results support the hypothesis that clearer lakes are more sensitive to climate variability and suggest that the relationship between lake color and climate sensitivity is nonlinear (Fig. 5a). These results also suggest that DOC acts as a buffer of water temperature against a warming climate. Thus, widespread increases in DOC observed in many regions (Monteith et al. 2007) may buffer or negate changes in water temperature resulting from anthropogically induced changes in climate. While these results are

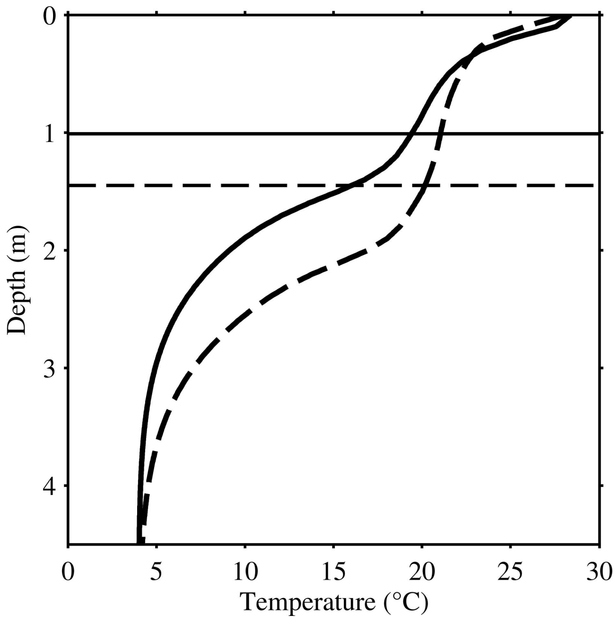

Fig. 6. Effects of transparency on mixed-layer depth. Trout Bog simulated water temperature for 01 July 2008 13:00 h using normal DOC concentrations (18.7 mg L^{-1}; black line) and a 50% DOC reduction scenario (dashed black line). Heat loss during the subsequent 15 h in each simulation eliminated near-surface microstratification, resulting in isothermal nocturnal mixed-layer depths of 1.01 and 1.45 m (black line and dashed black line, respectively). Meteorological drivers and starting conditions for the two simulations were identical.

specific to a certain lake type and geographic setting, the general pattern should hold for small lakes globally, although the absolute magnitude of these thermal ranges will vary as a function of lake depth and latitude (among other things). We expect that the effect of transparency as a regulator of climate will be amplified in regions with wider seasonal variations but muted in lakes of increasing volume. Darker lakes partition incoming solar radiation closer to the water surface, leading to larger outward energy fluxes and colder waters compared to clearer lakes. Conversely, clearer lakes integrate more of the climate signal into deeper waters both through less resistance to vertical mixing and through deeper penetration of incoming solar radiation. These lakes are therefore likely to be more sensitive to variations in climate.

The depth of the mixed layer is important in structuring aquatic ecosystems, and lake transparency (and DOC concentration) has been linked to mixed-layer depths for a variety of lakes (Kling 1988; Fee et al. 1996; Perez-Fuentetaja et al. 1999). Many investigators have proposed a simple mechanism for this finding, assuming that increased attenuation in darker waters creates a stronger density gradient that reduces wind-driven mixed-layer deepening (Kling 1988). However, wind is not as important as convection in regulating mixed-layer dynamics of very small lakes (Read et al. 2012). This distinction is important for small lakes, as scenarios of decreasing diel variability in air temperatures (which would likely result in less nocturnal heat loss) may lead to reduced mixed-layer depths even during periods of increasing wind speeds. Instead, the vertical partitioning of heat, not the differential resistance to wind-driven mixing, is more likely to be responsible for the observed relationship between mixed-layer depth and transparency. The effect of the vertical partitioning of heat on mixed-layer depth can be observed in Trout Bog simulations. In the normal (18.7 mg L^{-1}; Table 1) DOC scenario for 2008, heat loss created a (nighttime) convectively mixed layer that was 1.01 m deep on 01 July. In contrast, the 50% DOC reduction scenario mixed down to 1.45 m during the same period while losing 7% less heat compared to the normal case (Fig. 6). Thus, despite losing 7% less energy from the lake, the mixing depth of the 50% DOC reduction simulation was 44% deeper compared to the normal case. This difference is evident throughout the stratified period, as the temporally averaged 15 June–15 August 2008 mixed-layer depths (calculated at sunrise for comparison) were 0.85 and 1.4 m for the normal DOC and 50% reduction scenarios, respectively. This mechanism is likely responsible for the empirical relationship between transparency and epilimnetic depths for small, sheltered lakes (Fee et al. 1996).

While the magnitude of DOC change modeled here was large (a 50% increase and a 50% decrease), it is within the range observed in many regions. For example, Striegl et al. (2005) observed a 40% reduction in DOC export in the Yukon between growing seasons 1978–1980 and 2001–2003, and Schindler et al. (1992) observed over a 50% reduction in catchment DOC export during periods of drought compared with predrought conditions. Elsewhere, increases in DOC concentration have been reported. For example, Eimers et al. (2008) reported a 52–72% increase in DOC concentrations in small Canadian streams, and Evans et al. (2006) documented a 91% average increase in DOC concentrations across the United Kingdom. Thus, the change in transparency, mixed-layer depths, and volumetric temperatures modeled here are within the range that may be currently occurring in many regions.

Changes in DOC due to, for example, climatically induced reductions in catchment export of DOC may precipitate positive biological and photochemical feedbacks regulating DOC mineralization rates to rapidly alter DOC concentrations in small lakes. DOC mineralization rates increase with increasing temperatures, mixed-layer depths, and residence times (Hanson et al. 2011). Thus, as DOC concentrations are increased, lakes decrease in volumetrically averaged temperature and stratify more shallowly, and this can depress biological mineralization rates to further increase DOC concentrations. The opposite feedback could be occurring in regions experiencing decreased DOC loading, where longer water residence times and more transparent water facilitate greater biological and photochemical mineralization, further reducing DOC concentrations.

Small lakes play a disproportionately large role in the global carbon budget (Cole et al. 2007; Tranvik et al. 2009), and these lakes may be more sensitive to changes in hydrologic fluxes compared to larger lakes. For small temperate lakes, we have shown that water temperatures and mixed-layer depths are controlled by transparency, and dark lakes are less thermally sensitive to climate variability. Because of the potential for increases in DOC to buffer the thermal response of lakes to increases in air temperatures, investigators should consider linkages between climate and DOC loading when predicting the future role of small lakes in the global carbon budget.

Acknowledgments

J.S.R. was supported by National Science Foundation (NSF) North Temperate Lakes Long-Term Ecological Research grants from the Division of Environmental Biology and Molecular and Cellular Biology (grants 0822700 and 0702395, respectively). These grants also funded buoys on Crystal Bog, North Sparkling Bog, Trout Bog, and Mouser Bog. K.C.R. was supported by the Environmental Aquatic Resource Sensing (EARS) Integrative Graduate Education and Research Traineeship (IGERT) program, NSF Division of Graduate Education grant 0903560, and a Smithsonian Institution postdoctoral fellowship. The EARS IGERT grant supplied buoys for Timber and Jekl Bogs. This research could not have been completed without the intellectual and logistical support of the C. Williamson Lab of Miami University and the support, discussion, and/or fieldwork of K. McMahon, E. Stanley, L. Winslow, P. Hanson, E. K. Read, A. Shade, T. Meinke, K. Morrison, S. Yeo, and C. Watras. This article was improved by incorporating valuable feedback received at the 11th Global Lakes Ecological Observatory (GLEON) meeting, where travel and lodging costs for JSR and KCR were covered by the Gordon and Betty Moore Foundation (award 1182). We thank J. Cole and S. Carpenter from the Tropic Cascade Project for providing buoy data from Peter and Ward Lakes and M. Pace and R. Batt for thoughtful discussion on this topic. C. Williamson and two anonymous reviewers helped improve earlier versions of this article.

References

Carpenter, S. R., J. J. Cole, J. F. Kitchell, and M. L. Pace. 1998. Impact of dissolved organic carbon, phosphorus, and grazing on phytoplankton biomass and production in experimental lakes. Limnol. Oceanogr. **43:** 73–80, doi:10.4319/lo.1998.43.1.0073

Cole, J. J., S. R. Carpenter, J. Kitchell, M. L. Pace, C. T. Solomon, and B. Weidel. 2011. Strong evidence for terrestrial support of zooplankton in small lakes based on stable isotopes of carbon, nitrogen, and hydrogen. Proc. Natl. Acad. Sci. USA **108:** 1975–1980, doi:10.1073/pnas.1012807108

———, and others. 2007. Plumbing the global carbon cycle: Integrating inland waters into the terrestrial carbon budget. Ecosystems **10:** 171–184, doi:10.1007/s10021-006-9013-8

Destasio, B. T., D. K. Hill, J. M. Kleinhans, N. P. Nibbelink, and J. J. Magnuson. 1996. Potential effects of global climate change on small north-temperate lakes: Physics, fish, and plankton. Limnol. Oceanogr. **41:** 1136–1149, doi:10.4319/lo.1996.41.5.1136

Downing, J. A. 2010. Emerging global role of small lakes and ponds: Little things mean a lot. Limnetica **29:** 9–23.

———, and others. 2006. The global abundance and size distribution of lakes, ponds, and impoundments. Limnol. Oceanogr. **51:** 2388–2397, doi:10.4319/lo.2006.51.5.2388

Eimers, M. C., S. A. Watmough, and J. M. Buttle. 2008. Long-term trends in dissolved organic carbon concentration: A cautionary note. Biogeochemistry **87:** 71–81, doi:10.1007/s10533-007-9168-1

Evans, C. D., P. J. Chapman, J. M. Clark, D. T. Monteith, and M. S. Cresser. 2006. Alternative explanations for rising dissolved organic carbon export from organic soils. Glob. Change Biol. **12:** 2044–2053, doi:10.1111/j.1365-2486.2006.01241.x

Fee, E. J., R. E. Hecky, S. E. M. Kasian, and D. R. Cruikshank. 1996. Effects of lake size, water clarity, and climatic variability on mixing depths in Canadian Shield lakes. Limnol. Oceanogr. **41:** 912–920, doi:10.4319/lo.1996.41.5.0912

Hanson, P. C., D. P. Hamilton, E. H. Stanley, N. Preston, O. C. Langman, and E. L. Kara. 2011. Fate of allochthonous dissolved organic carbon in lakes: A quantitative approach. PLoS One **6:** e21884, doi:10.1371/journal.pone.0021884

Imberger, J. 1985. The diurnal mixed layer. Limnol. Oceanogr. **30:** 737–770, doi:10.4319/lo.1985.30.4.0737

———, and J. C. Patterson. 1981. A dynamic reservoir simulation model- DYRESM 5, p. 310–361. *In* H. B. Fischer [ed.], Transport models for inland and coastal waters. Academic Press.

Jennings, E., and others. 2010. Impacts of climate on the flux of dissolved organic carbon from catchments, p. 199–220. *In* D. G. George [ed.], The impact of climate change on European lakes. Springer.

Kirk, J. T. O. 1994. Light and photosynthesis in aquatic ecosystems, 2nd ed. Cambridge University Press.

Kling, G. W. 1988. Comparative transparency, depth of mixing, and stability of stratification in lakes of Cameroon, West-Africa. Limnol. Oceanogr. **33:** 27–40, doi:10.4319/lo.1988.33.1.0027

Markfort, C. D., A. L. S. Perez, J. W. Thill, D. A. Jaster, F. Porte-Agel, and H. G. Stefan. 2010. Wind sheltering of a lake by a tree canopy or bluff topography. Water Resour. Res. **46:** W03530, doi:10.1029/2009WR007759

Mazumder, A., and W. D. Taylor. 1994. Thermal structure of lakes varying in size and water clarity. Limnol. Oceanog. **39:** 968–976, doi:10.4319/lo.1994.39.4.0968

Monteith, D. T., and others. 2007. Dissolved organic carbon trends resulting from changes in atmospheric deposition chemistry. Nature **450:** 537–539, doi:10.1038/nature06316

Morris, D. P., and others. 1995. The attentuation of solar UV radiation in lakes and the role of dissolved organic carbon. Limnol. Oceanogr. **40:** 1381–1391, doi:10.4319/lo.1995.40.8.1381

Pechar, L. 1987. Use of an acetone-methanol mixture for the extraction and spectrophotometric determination of chlorophyll *a* in pytoplankton. Arch. Hydrobiol. **78:** 99–117.

Perez-Fuentetaja, A., P. J. Dillon, N. D. Yan, and D. J. McQueen. 1999. Significance of dissolved organic carbon in the prediction of thermocline depth in small Canadian shield lakes. Aquat. Ecol. **33:** 127–133, doi:10.1023/A:1009998118504

Persson, I., and I. D. Jones. 2008. The effect of water colour on lake hydrodynamics: A modelling study. Freshw. Biol. **53:** 2345–2355, doi:10.1111/j.1365-2427.2008.02049.x

Rasmussen, A. H., M. Hondzo, and H. G. Stefan. 1995. A test of several evaporation equations for water temperature simulations in lakes. Water Resour. Bull. **31:** 1023–1028, doi:10.1111/j.1752-1688.1995.tb03418.x

Read, J. S., A. Shade, C. H. Wu, A. Gorzalski, and K. D. McMahon. 2011. "Gradual entrainment lake inverter" (GELI): A novel device for experimental lake mixing. Limnol. Oceanogr.: Methods **9:** 14–28, doi:10.4319/lom.2011.9.14

———, and others. 2012. Lake-size dependency of wind shear and convection as controls on gas exchange. Geophys. Res. Lett. **39:** L09405, doi:10.1029/2012gl051886

Rose, K. C., C. E. Williamson, J. E. Saros, R. Sommaruga, and J. M. Fischer. 2009*a*. Differences in UV transparency and thermal structure between alpine and subalpine lakes: Implications for organisms. Photochem. Photobiol. Sci. **8:** 1244–1256, doi:10.1039/b905616e

———, ———, S. G. Schladow, M. Winder, and J. T. Oris. 2009*b*. Patterns of spatial and temporal variability of UV transparency in Lake Tahoe, California-Nevada. J. Geophys. Res. Biogeosci. **114:** G00D03, doi:10.1029/2008jg000816

Schindler, D. W., S. E. Bayley, P. J. Curtis, B. R. Parker, M. P. Stainton, and C. A. Kelly. 1992. Natural and man-caused factors affecting the abundance and cycling of dissolved organic substances in precambrian shield lakes. Hydrobiologia **229:** 1–21, doi:10.1007/BF00006987

———, and others. 1996. The effects of climatic warming on the properties of boreal lakes and streams at the Experimental Lakes Area, northwestern Ontario. Limnol. Oceanogr. **41:** 1004–1017, doi:10.4319/lo.1996.41.5.1004

Snucins, E., and J. Gunn. 2000. Interannual variation in the thermal structure of clear and colored lakes. Limnol. Oceanogr. **45:** 1639–1646, doi:10.4319/lo.2000.45.7.1639

Striegl, R. G., G. R. Aiken, M. M. Dornblaser, P. A. Raymond, and K. P. Wickland. 2005. A decrease in discharge-normalized DOC export by the Yukon River during summer through autumn. Geophys. Res. Lett. **32:** L21413, doi:10.1029/2005gl024413

Tranvik, L. J., and others. 2009. Lakes and reservoirs as regulators of carbon cycling and climate. Limnol. Oceanogr. **54:** 2298–2314, doi:10.4319/lo.2009.54.6_part_2.2298

Williamson, C. E., R. S. Stemberger, D. P. Morris, T. M. Frost, and S. G. Paulsen. 1996. Ultraviolet radiation in North American lakes: Attenuation estimates from DOC measurements and implications for plankton communities. Limnol. Oceanogr. **41:** 1024–1034, doi:10.4319/lo.1996.41.5.1024

Zhang, J., and others. 2010. Long-term patterns of dissolved organic carbon in lakes across eastern Canada: Evidence of a pronounced climate effect. Limnol. Oceanogr. **55:** 30–42, doi:10.4319/lo.2010.55.1.0030

Associate editor: George W. Kling

Received: 5 April 2012
Accepted: 03 December 2012
Amended: 01 February 2013